# Computational algorithms derived from multiple scales of neocortical processing

**Lester Ingber**

**Lester Ingber Research**
**Ashland Oregon USA**
**ingber@ingber.com, ingber@alumni.caltech.edu**
**http://www.ingber.com/**

## Abstract

A statistical mechanics of neocortical interactions (SMNI) of columnar activity, and the vector potential of minicolumnar electromagnetic activity, provide a context to explore neocortical information processes and influences on cognitive processing at multiple scales, i.e., mesoscopic (columnar scales), macroscopic (mesoscopic influences at regional scales), and microscopic (mesoscopic influences of ions affecting interactions between and among neurons and astrocytes). Even within this confined context, a case has been made that it should not be expected that the proposed Holy Grail of neuroscience, i.e., to ultimately explain all brain processing in terms of a nonlinear science at molecular scales, is at all realistic. As with many Crusades for some truths, other truths can be trampled.

---

Most recent drafts are available as http://www.ingber.com/smni12_cog_comp.pdf

$Id: smni11_cog_comp,v 1.18 2011/07/05 23:24:43 ingber Exp $

## 1. Introduction

There many kinds of cognitive computation discovered and proposed in neocortex (Grossberg, 1983; Arbib & Amari, 1985; Hagan *et al*, 2002; Naruse *et al*, 2009; Pereira & Furlan, 2010; Banaclocha, Bóokkon & Banaclocha, 2010; Anastassiou *et al*, 2011). Here, primarily short-term memory (STM) processes are considered, as described and calculated in a series of statistical mechanics of neocortical interactions (SMNI) papers. In the next Section, a short description is given of how SMNI aggregates synaptic and neuronal processes into mesoscopic minicolumnar and macrocolumnar processes, and how STM is derived. A sub-Section describes applications to artificial intelligence and to biologically-inspired computational algorithms. In the following Section after, a description is given of how these relatively mesoscopic processes affect and are affected by relatively macroscopic regional processes. An example is given of SMNI calculations developing specific analysis to EEG data. In the next Section after, a description is given of how these relatively mesoscopic processes affect and are affected by relatively microscopic ionic processes, influencing astrocyte and astrocyte-neuronal interactions. The last Section is a summary and conclusion.

## 2. Mesoscales

Neocortex has evolved to use minicolumns of neurons interacting via short-ranged interactions in macrocolumns, and interacting via long-ranged interactions across regions of macrocolumns (Mountcastle, 1978; Buxhoeveden & Casanova, 2002; Rakic, 2008). This common architecture processes patterns of information within and among different regions of sensory, motor, associative cortex, etc. Such probability distributions are a basic input into the approach used here. The statistical mechanics of neocortical interactions (SMNI) approach was the first physical application of a nonlinear multivariate calculus developed by other mathematical physicists in the late 1970's to define a statistical mechanics of multivariate nonlinear nonequilibrium systems (Graham, 1977; Langouche *et al*, 1982).

### 2.1. SMNI Tests on STM and EEG

SMNI builds minicolumnar, macrocolumnar, and regional interactions in neocortex. Since 1981, SMNI has been developed to model columns and regions of neocortex, spanning mm to cm of tissue, As depicted in Figure 1, SMNI develops three biophysical scales of neocortical interactions: (a)-($a^*$)-(a') microscopic neurons; (b)-(b') mesocolumnar domains; (c)-(c') macroscopic regions. SMNI has developed appropriate conditional probability distributions at each level, aggregating up from the smallest levels of interactions. In ($a^*$) synaptic inter-neuronal interactions, averaged over by mesocolumns, are phenomenologically described by the mean and variance of a distribution $\Psi$. Similarly, in (a) intraneuronal transmissions are phenomenologically described by the mean and variance of $\Gamma$. Mesocolumnar averaged excitatory ($E$) and inhibitory ($I$) neuronal firings $M$ are represented in (a'). In (b) the vertical organization of minicolumns is sketched together with their horizontal stratification, yielding a physiological entity, the mesocolumn. In (b') the overlap of interacting mesocolumns at locations $r$ and $r'$ from times $t$ and $t + \tau$ is sketched. In (c) macroscopic regions of neocortex are depicted as arising from many mesocolumnar domains. (c') sketches how regions may be coupled by long−ranged interactions.

Most of these papers have dealt explicitly with calculating properties of STM and scalp EEG in order to test the basic formulation of this approach (Ingber, 1981; Ingber, 1982; Ingber, 1983; Ingber, 1984; Ingber, 1985b; Ingber, 1985c; Ingber, 1986; Ingber & Nunez, 1990; Ingber, 1991; Ingber, 1992; Ingber, 1994; Ingber & Nunez, 1995; Ingber, 1995a; Ingber, 1995b; Ingber, 1996b; Ingber, 1996a; Ingber, 1997; Ingber, 1998). The SMNI modeling of local mesocolumnar interactions (convergence and divergence between minicolumnar and macrocolumnar interactions) was tested on STM phenomena. The SMNI modeling of macrocolumnar interactions across regions was tested on EEG phenomena.

#### 2.1.1. SMNI Description of STM

SMNI studies have detailed that maximal numbers of attractors lie within the physical firing space of $M^G$, where $G$ = {Excitatory, Inhibitory} minicolumnar firings, consistent with experimentally observed capacities of auditory STM (Miller, 1956; Ericsson & Chase, 1982) and visual STM (Zhang & Simon, 1985), when a "centering" mechanism (CM) is enforced by shifting background noise in synaptic

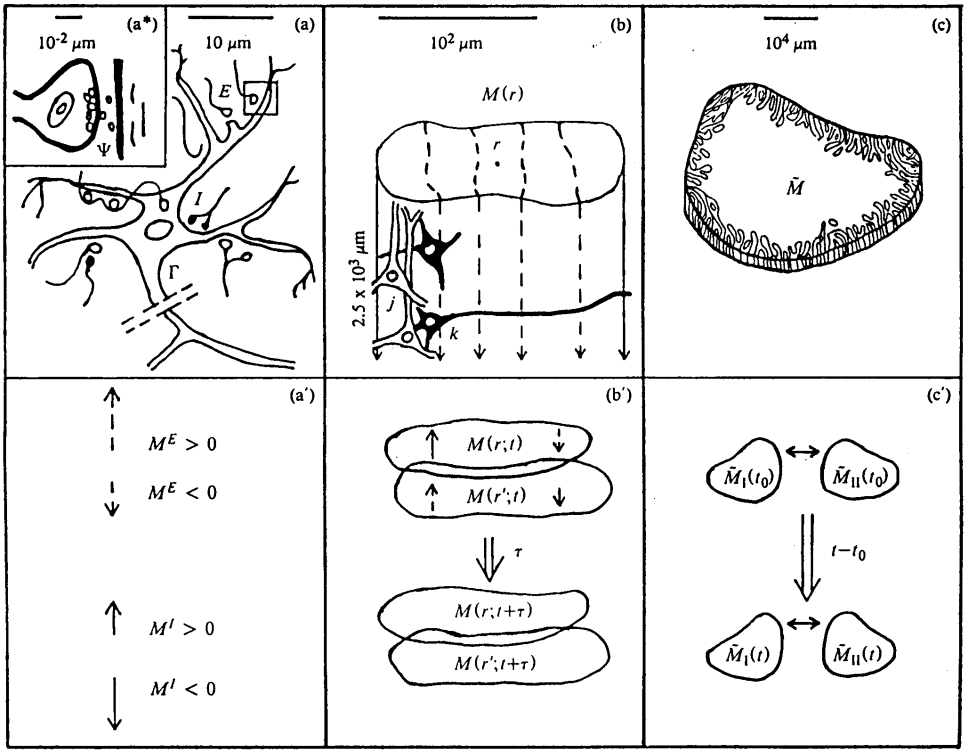


Fig. 1. Illustrated are three biophysical scales of neocortical interactions: (a)-(a*)-(a') microscopic neurons; (b)-(b') mesocolumnar domains; (c)-(c') macroscopic regions. Reprinted with permission from (Ingber, 1983) by the American Physical Society.

interactions, consistent with experimental observations under conditions of selective attention (Mountcastle *et al*, 1981; Ingber, 1984; Ingber, 1985c; Ingber, 1994; Ingber & Nunez, 1995). This leads to all attractors of the short-time distribution lying along a diagonal line in $M^G$ space, effectively defining a narrow parabolic trough containing these most likely firing states. This essentially collapses the 2 dimensional $M^G$ space down to a one-dimensional space of most importance. Thus, the predominant physics of STM and of (short-fiber contribution to) EEG phenomena takes place in a narrow "parabolic trough" in $M^G$ space, roughly along a diagonal line (Ingber, 1984).

These calculations were further supported by high-resolution evolution of the two-variable short-time conditional-probability propagator using PATHINT (Ingber & Nunez, 1995). SMNI correctly calculated the stability and duration of STM, the primacy versus recency rule, random access to memories within tenths of a second as observed, and the observed $7 \pm 2$ capacity rule of auditory memory and the observed $4 \pm 2$ capacity rule of visual memory.

SMNI also calculates how STM patterns (e.g., from a given region or even aggregated from multiple regions) may be encoded by dynamic modification of synaptic parameters (within experimentally observed ranges) into long-term memory patterns (LTM) (Ingber, 1983).

### 2.1.2. Mathematical Development

Some of the algebra behind SMNI depicts variables and distributions that populate each representative macrocolumn in each region.

A derived mesoscopic Lagrangian $\underline{L}_M$ defines the short-time probability distribution of firings in a minicolumn, composed of about $10^2$ neurons, given its just previous interactions with all other neurons in its macrocolumnar surround. $G$ is used to represent excitatory ($E$) and inhibitory ($I$) contributions. $\bar{G}$ designates contributions from both $E$ and $I$.

$$P_M = \prod_G P_M^G[M^G(r;t+\tau)|M^{\bar{G}}(r';t)]$$

$$= \sum_{\sigma_j} \delta\left( \sum_{jE} \sigma_j - M^E(r;t+\tau) \right) \delta\left( \sum_{jI} \sigma_j - M^I(r;t+\tau) \right) \prod_j^N p_{\sigma_j}$$

$$\approx \prod_G (2\pi\tau g^{GG})^{-1/2} \exp(-N\tau \underline{L}_M^G) \, ,$$

$$P_M \approx (2\pi\tau)^{-1/2} g^{1/2} \exp(-N\tau \underline{L}_M) \, ,$$

$$\underline{L}_M = \underline{L}_M^E + \underline{L}_M^I = (2N)^{-1}(\dot{M}^G - g^G) g_{GG'} (\dot{M}^{G'} - g^{G'}) + M^G J_G/(2N\tau) - \underline{V}' \, ,$$

$$\underline{V}' = \sum_G \underline{V}''^G_{G'} (\rho \nabla M^{G'})^2 \, ,$$

$$g^G = -\tau^{-1}(M^G + N^G \tanh F^G) \, , \; g^{GG'} = (g_{GG'})^{-1} = \delta^{G'}_G \tau^{-1} N^G \mathrm{sech}^2 F^G \; , \; g = \det(g_{GG'}) \, ,$$

$$F^G = \frac{(V^G - a^{|G|}_{G'} v^{|G|}_{G'} N^{G'} - \frac{1}{2} A^{|G|}_{G'} v^{|G|}_{G'} M^{G'})}{\left((\pi/2)[(v^{|G|}_{G'})^2 + (\phi^{|G|}_{G'})^2](a^{|G|}_{G'} N^{G'} + \frac{1}{2} A^{|G|}_{G'} M^{G'})\right)^{1/2}} \, , a^G_{G'} = \frac{1}{2} A^G_{G'} + B^G_{G'} \, , \tag{1}$$

where $A^G_{G'}$ and $B^G_{G'}$ are minicolumnar-averaged inter-neuronal synaptic efficacies, $v^G_{G'}$ and $\phi^G_{G'}$ are averaged means and variances of contributions to neuronal electric polarizations. $M^{G'}$ and $N^{G'}$ in $F^G$ are afferent macrocolumnar firings, scaled to efferent minicolumnar firings by $N/N^* \approx 10^{-3}$, where $N^*$ is the number of neurons in a macrocolumn, about $10^5$. Similarly, $A^{G'}_G$ and $B^{G'}_G$ have been scaled by $N^*/N \approx 10^3$ to keep $F^G$ invariant. $\underline{V}'$ are mesocolumnar nearest-neighbor interactions.

### 2.1.3. Inclusion of Macroscopic Circuitry

The most important features of this development are described by the Lagrangian $\underline{L}^G$ in the negative of the argument of the exponential describing the probability distribution, and the "threshold factor" $F^G$ describing an important sensitivity of the distribution to changes in its variables and parameters.

To more properly include long-ranged fibers, when it is possible to numerically include interactions among macrocolumns, the $J_G$ terms can be dropped, and more realistically replaced by a modified threshold factor $F^G$,

$$F^G = \frac{(V^G - a^{|G|}_{G'} v^{|G|}_{G'} N^{G'} - \frac{1}{2} A^{|G|}_{G'} v^{|G|}_{G'} M^{G'} - a^{\ddagger E}_{E'} v^E_{E'} N^{\ddagger E'} - \frac{1}{2} A^{\ddagger E}_{E'} v^E_{E'} M^{\ddagger E'})}{\left((\pi/2)[(v^{|G|}_{G'})^2 + (\phi^{|G|}_{G'})^2](a^{|G|}_{G'} N^{G'} + \frac{1}{2} A^{|G|}_{G'} M^{G'} + a^{\ddagger E}_{E'} N^{\ddagger E'} + \frac{1}{2} A^{\ddagger E}_{E'} M^{\ddagger E'})\right)^{1/2}} \, ,$$

$$a^{\ddagger E}_{E'} = \frac{1}{2} A^{\ddagger E}_{E'} + B^{\ddagger E}_{E'} \, . \tag{2}$$

Here, afferent contributions from $N^{\ddagger E}$ long-ranged excitatory fibers, e.g., cortico-cortical neurons, have been added, where $N^{\ddagger E}$ might be on the order of 10% of $N^*$: Of the approximately $10^{10}$ to $10^{11}$ neocortical neurons, estimates of the number of pyramidal cells range from 2/3 up to 4/5. Nearly every pyramidal cell has an axon branch that makes a cortico-cortical connection; i.e., the number of cortico-cortical fibers is of the order $10^{10}$.

### 2.1.4. Centering Mechanism (CM)

It was discovered that more minima of the static Lagrangian $\bar{L}$ are created, i.e., brought into the physical firing ranges, if the numerator of $F^G$ contains terms only in $\bar{M}^G$, tending to center $\bar{L}$ about $\bar{M}^G = 0$ (Ingber, 1984). That is, $B^G$ is modified such that the numerator of $F^G$ is transformed to

$$F'^{G} = \frac{-\frac{1}{2} A^{|G|}_{G'} v^{|G|}_{G'} M^{G'}}{((\pi/2)[(v^{|G|}_{G'})^2 + (\phi^{|G|}_{G'})^2](a'^{|G|}_{G'} N^{G'} + \frac{1}{2} A^{|G|}_{G'} M^{G'}))^{1/2}} ,$$

$$a'^{G}_{G'} = \frac{1}{2} A^{G}_{G'} + B'^{G}_{G'} , \tag{3}$$

The most likely states of the centered systems lie along diagonals in $M^G$ space, a line determined by the numerator of the threshold factor in $F^E$, essentially

$$A^E_E M^E - A^E_I M^I \approx 0 , \tag{4}$$

noting that in $F^I$ $I - I$ connectivity is experimentally observed to be very small relative to other pairings, so that $(A^I_E M^E - A^I_I M^I)$ is typically small only for small $M^E$.

Of course, any mechanism producing more as well as deeper minima is statistically favored. However, this particular CM has plausible support: $M^G(t+\tau) = 0$ is the state of afferent firing with highest statistical weight. I.e., there are more combinations of neuronal firings, $\sigma_j = \pm 1$, yielding this state than any other $M^G(t+\tau)$, e.g., $\approx 2^{N^G+1/2}(\pi N^G)^{-1/2}$ relative to the states $M^G = \pm N^G$. Similarly, $M^G(t)$ is the state of efferent firing with highest statistical weight. Therefore, it is natural to explore mechanisms which favor common highly weighted efferent and afferent firings in ranges consistent with favorable firing threshold factors $F^G \approx 0$.

In general, $B^G_E$ and $B^G_I$ (and possibly $A^G_E$ and $A^G_I$ due to actions of neuromodulators, and $J_G$ constraints from long-ranged fibers) are available to zero the constant in the numerator, giving an extra degree(s) of freedom to this mechanism. (If $B'^G_E$ would be negative, this leads to unphysical results in the square-root denominator of $F^G$. In all examples where this occurs, it is possible to instead find positive $B'^G_I$ to appropriately shift the numerator of $F^G$.) In this context, it is empirically observed that the synaptic sensitivity of neurons engaged in selective attention is altered, presumably by the influence of chemical neuromodulators on postsynaptic neurons at their presynaptic sites (Mountcastle *et al*, 1981).

### 2.2. Computational Physics

#### 2.2.1. Adaptive Simulated Annealing (ASA)

Adaptive Simulated Annealing (ASA) (Ingber, 1993) is used to optimize or importance-sample parameters of systems.

ASA is a C-language code developed to statistically find the best global fit of a nonlinear constrained non-convex cost-function over a $D$-dimensional space. This algorithm permits an annealing schedule for "temperature" $T$ decreasing exponentially in annealing-time $k$, $T = T_0 \exp(-ck^{1/D})$. The introduction of re-annealing also permits adaptation to changing sensitivities in the multi-dimensional parameter-space. This annealing schedule is faster than fast Cauchy annealing, where $T = T_0/k$, and much faster than Boltzmann annealing, where $T = T_0/\ln k$. ASA has over 100 OPTIONS to provide robust tuning over many classes of nonlinear stochastic systems.

For example, ASA has ASA_PARALLEL OPTIONS, hooks to use ASA on parallel processors, which were first developed in 1994 when the author was Principal Investigator (PI) of a National Science Foundation grant, Parallelizing ASA and PATHINT Project (PAPP). Since then these OPTIONS have been used by people in various institutions.

#### 2.2.2. PATHINT and PATHTREE

In some cases, it is desirable to develop a time evolution of a short-time conditional probability. Two useful algorithms have been developed and published by the author.

PATHINT (Ingber, 1994) motivated the development of PATHTREE (Ingber, Chen *et al*, 2001), an algorithm that permits extremely fast accurate computation of probability distributions of a large class of general nonlinear diffusion processes.

The natural metric of the space is used to first lay down the mesh. The evolving local short-time distributions on this mesh are then dynamically calculated. The short-time probability density gives the correct result up to order $O(\Delta t)$ for any final point $S'$, the order required to recover the corresponding partial differential equation. In fact, $O(\Delta t^{3/2})$ is available (Graham, 1978; Langouche *et al*, 1979; Langouche *et al*, 1982).

PATHINT and PATHTREE have demonstrated their utility in statistical mechanical studies in finance, neuroscience, combat analyses, neuroscience, and other selected nonlinear multivariate systems (Ingber, Fujio & Wehner, 1991; Ingber & Nunez, 1995; Ingber, 2000). PATHTREE has been used extensively to price financial options (Ingber, Chen *et al*, 2001).

### 2.3. Mesoscopic Computation

#### 2.3.1. Generic Mesoscopic Neural Networks (MNN)

SMNI was applied to a parallelized generic mesoscopic neural networks (MNN) (Ingber, 1992), adding computational power to a similar paradigm proposed for target recognition (Ingber, 1985a).

"Learning" takes place by presenting the MNN with data, and parametrizing the data in terms of the firings, or multivariate firings. The "weights," or coefficients of functions of firings appearing in the drifts and diffusions, are fit to incoming data, considering the joint "effective" Lagrangian (including the logarithm of the prefactor in the probability distribution) as a dynamic cost function. This program of fitting coefficients in Lagrangian uses methods of ASA.

"Prediction" takes advantage of a mathematically equivalent representation of the Lagrangian path-integral algorithm, i.e., a set of coupled Langevin rate-equations. A coarse deterministic estimate to "predict" the evolution can be applied using the most probable path, but PATHINT has been used. PATHINT, even when parallelized, typically can be too slow for "predicting" evolution of these systems. However, PATHTREE is much faster.

The present project uses the same concepts, having sets of multiple variables define macrocolumns with a region, with long-ranged connectivity to other regions. Each macrocolumn has its own parameters, which define sets of possible patterns.

#### 2.3.2. Ideas by Statistical Mechanics (ISM)

These kinds of applications of SMNI have obvious counterparts in an AI approach to Ideas by Statistical Mechanics (ISM). ISM is a generic program to model evolution and propagation of ideas/patterns throughout populations subjected to endogenous and exogenous interactions. The program is based on the author's work in SMNI, and uses the author's ASA code (Ingber, 1993) for optimizations of training sets, as well as for importance-sampling to apply the author's copula financial risk-management codes, TRD (Ingber, 2005), for assessments of risk and uncertainty. This product can be used for decision support for projects ranging from diplomatic, information, military, and economic (DIME) factors of propagation/evolution of ideas, to commercial sales, trading indicators across sectors of financial markets, advertising and political campaigns, etc.

It seems appropriate to base an approach for propagation of ideas on the only system so far demonstrated to develop and nurture ideas, i.e., the neocortical brain (Ingber, 2006; Ingber, 2007; Ingber, 2008). Ultimately, ISM of course would not use functional relationships developed solely in neocortex, but rather those more appropriate to a given population.

Following the SMNI structure, ISM develops subsets of macrocolumnar activity of multivariate stochastic descriptions of defined populations, with macrocolumns defined by their local parameters within specific regions and with parameterized endogenous inter-regional and exogenous external connectivities. Parameters of subsets of macrocolumns are to be fit using ASA to patterns representing ideas. Parameters of external and inter-regional interactions are to be determined that promote or inhibit the spread of these ideas.

## 3. Macroscales

### 3.1. SMNI Description of EEG

Using the power of the SMNI structure and ASA, sets of EEG and evoked potential data from a separate NIH study, collected to investigate genetic predispositions to alcoholism, were fitted to an SMNI model on a lattice of regional electrodes to extract brain "signatures" of STM (Ingber, 1997; Ingber, 1998). Each electrode site was represented by an SMNI distribution of independent stochastic macrocolumnar-scaled $M^G$ variables, interconnected by long-ranged circuitry with delays appropriate to long-fiber communication in neocortex. The global optimization algorithm ASA was used to perform maximum likelihood fits of Lagrangians defined by path integrals of multivariate conditional probabilities. Canonical momenta indicators (CMI) were thereby derived for individual's EEG data. The CMI give better signal recognition than the raw data, and were used to advantage as correlates of behavioral states. In-sample data was used for training (Ingber, 1997), and out-of-sample data was used for testing (Ingber, 1998) these fits.

These results gave strong quantitative support for an accurate intuitive picture, portraying neocortical interactions as having common algebraic physics mechanisms that scale across quite disparate spatial scales and functional or behavioral phenomena, i.e., describing interactions among neurons, columns of neurons, and regional masses of neurons.

### 3.2. Complementary Global Models of EEG

There are other models of EEG which also have sound experimental support. Some of the models can be shown to be indeed complementary to SMNI (Ingber & Nunez, 2010). Scalp potentials (EEG) are generated by synaptic current sources at small scales; each cubic millimeter of cortical tissue contains more than 100 million synapses. In contrast to this small scale activity, EEG data are recorded at macroscopic (centimeter) scales. All dependent variables are expressed as functions of time and cortical location. The basic approach ignores embedded network activity, although networks have been included in more advanced models (Nunez, 1989; Jirsa & Haken, 1996).

#### 3.2.1. The Stretched String With Attached Springs

Periodic boundary conditions are generally essential to global theories because the cortical-white matter system is topologically close to a spherical shell. While this picture of distinct local and global models grossly oversimplifies expected genuine dynamic behaviors with substantial cross- scale interactions, it provides a convenient entry point to brain complexity (Nunez, 1995; Ingber, 1995a). In the "string model" displacement is governed by the basic string equation

$$\frac{\partial^2 \Phi}{\partial t^2} - v^2 \frac{\partial^2 \Phi}{\partial x^2} + [\omega_0^2 + f(\Phi)]\Phi = 0 \tag{5}$$

For the simple case of homogeneous linear springs attached to a homogeneous linear string of length $a$ and wave speed $v$, the normal modes of oscillation $\omega_n$ are given by

$$\omega_n^2 = \omega_0^2 + (\frac{n\pi v}{a})^2 \qquad n = 1, 2, 3, \ldots \tag{6}$$

### 3.3. SMNI Derivation of String Model

#### 3.3.1. Euler-Lagrange (EL)

The EL equations are derived from the long-time conditional probability distribution of columnar firings over all cortex, represented by $\tilde{M}$, in terms of the Action $S$, The path integral has a variational principle, $\delta L = 0$ which gives the EL equations for SMNI (Ingber, 1982; Ingber, 1983).

When dealing when multivariate Gaussian stochastic systems with nonlinear drifts and diffusions, it is possible to work with three essentially mathematically equivalent representations of the same physics: Langevin equations — coupled stochastic differential equations, a Fokker-Plank equation — a

multivariate partial differential equation, and a path-integral Lagrangian — detailing the evolution of the short-time conditional probability distribution of the variables (Langouche *et al*, 1982).

While it typically takes more numerical and algebraic expertise to deal with the path-integral Lagrangian, there are many benefits, including intuitive numerical and algebraic tools. For example, the Lagrangian components and EL equations are essentially the counterpart to classical dynamics,

$$\text{Mass} = g_{GG'} = \frac{\partial^2 L}{\partial(\partial M^G/\partial t)\partial(\partial M^{G'}/\partial t)} ,$$

$$\text{Momentum} = \Pi^G = \frac{\partial L}{\partial(\partial M^G/\partial t)} ,$$

$$\text{Force} = \frac{\partial L}{\partial M^G} ,$$

$$\text{F} - \text{ma} = 0: \ \delta L = 0 = \frac{\partial L}{\partial M^G} - \frac{\partial}{\partial t}\,\frac{\partial L}{\partial(\partial M^G/\partial t)} \tag{7}$$

The most-probable firing states derived variationally from the path-integral Lagrangian as the EL equations represent a reasonable average over the noise in the SMNI system. For many studies, the noise cannot be simply disregarded, as demonstrated in other SMNI STM and EEG studies, but for the purpose here of demonstrating the existence of multiple local oscillatory states that can be identified with EEG frequencies, the EL equations serve very well.

The Lagrangian and associated EL equations have been developed at SMNI columnar scales, as well as for regional scalp EEG activity by scaling up from the SMNI columnar scales as outlined below.

### 3.3.2. Strings

The nonlinear string model was derived using the EL equation for the electric potential $\Phi$ measured by EEG, considering one firing variable along the parabolic trough of attractor states being proportional to $\Phi$ (Ingber & Nunez, 1990).

Since only one variable, the electric potential is being measured, is reasonable to assume that a single independent firing variable offers a crude description of this physics. Furthermore, the scalp potential $\Phi$ can be considered to be a function of this firing variable. (Here, "potential" refers to the electric potential, not any potential term in the SMNI Lagrangian.) In an abbreviated notation subscripting the time-dependence,

$$\Phi_t - \ll \Phi \gg = \Phi(M_t^E, M_t^I) \approx a(M_t^E - \ll M^E \gg) + b(M_t^I - \ll M^I \gg) , \tag{8}$$

where $a$ and $b$ are constants, and $\ll \Phi \gg$ and $\ll M^G \gg$ represent typical minima in the trough. In the context of fitting data to the dynamic variables, there are three effective constants, $\{ a, b, \phi \}$ ,

$$\Phi_t - \phi = aM_t^E + bM_t^I \tag{9}$$

The mesoscopic columnar probability distributions, $P$, is scaled over this columnar firing space to obtain the macroscopic conditional probability distribution over the scalp-potential space:

$$P_\Phi[\Phi] = \int dM^E dM^I P[M^E, M^I]\delta[\Phi - \Phi'(M^E, M^I)] \tag{10}$$

The parabolic trough described above justifies a form

$$P_\Phi = (2\pi\sigma^2)^{-1/2} \exp(-\Delta t \int dx\, L_\Phi) ,$$

$$L_\Phi = \frac{\alpha}{2}\,|\partial\Phi/\partial t|^2 + \frac{\beta}{2}\,|\partial\Phi/\partial x|^2 + \frac{\gamma}{2}\,|\Phi|^2 + F(\Phi) ,$$

$$\sigma^2 = 2\Delta t/\alpha , \tag{11}$$

where $F(\Phi)$ contains nonlinearities away from the trough, $\sigma^2$ is on the order of $1/N$ given the derivation of $\underline{L}$ above, and the integral over $x$ is taken over the spatial region of interest. In general, there also will be terms linear in $\partial\Phi/\partial t$ and in $\partial\Phi/\partial x$.

Here, the EL equation includes variation across the spatial extent, $x$, of columns in regions,

$$\frac{\partial}{\partial t}\frac{\partial L}{\partial(\partial\Phi/\partial t)}+\frac{\partial}{\partial x}\frac{\partial L}{\partial(\partial\Phi/\partial x)}-\frac{\partial L}{\partial\Phi}=0 \tag{12}$$

The result is

$$\alpha\frac{\partial^2\Phi}{\partial t^2}+\beta\frac{\partial^2\Phi}{\partial x^2}+\gamma\Phi-\frac{\partial F}{\partial\Phi}=0 \tag{13}$$

The determinant prefactor $g$ defined above also contains nonlinear details affecting the state of the system. Since $g$ is often a small number, distortion of the scale of $L$ is avoided by normalizing $g/g_0$, where $g_0$ is simply $g$ evaluated at $M^E = M^{\ddagger E'} = M^I = 0$.

If there exist regions in neocortical parameter space such that $\beta/\alpha = -c^2$, $\gamma/\alpha = \omega_0^2$, i.e., as explicitly calculated using the Centering Mechanism (CM) and as derived in previous SMNI EEG papers,

$$\frac{1}{\alpha}\frac{\partial F}{\partial\Phi}=-\Phi f(\Phi)\,, \tag{14}$$

then the nonlinear string model is recovered.

Note that this string derivation is only consistent with the global string analog described in the first sections of this paper, if the spatial extent is extended across the scalp via long-ranged fibers connecting columns with $M^{\ddagger E'}$ firings. This leads to a string of columns. The next section calculates an EL model that shows that these columns can be viewed as spring analogs.

### 3.3.3. Springs

For a given column in terms of the probability description given above, the above EL equations are represented as

$$\frac{\partial}{\partial t}\frac{\partial L}{\partial(\partial M^E/\partial t)}-\frac{\partial L}{\partial M^E}=0\,,$$

$$\frac{\partial}{\partial t}\frac{\partial L}{\partial(\partial M^I/\partial t)}-\frac{\partial L}{\partial M^I}=0 \tag{15}$$

Early calculations included many coupled equations, representing spatial and spatial-derivative terms in the Lagrangian from nearest-neighbor minicolumns. SMNI includes divergence and convergence of columnar interactions, whereby a minicolumn interacts afferently and efferently via its axonal processes to a subset of neuronal dentritic afferents as well as to other minicolumns, defining a dynamic mesocolumn (Ingber, 1982; Ingber, 1983). These spatial terms permit calculation and verification of observed velocities of propagation of information across minicolumns via short-ranged non-myelinated fibers.

To investigate dynamics of multivariate stochastic nonlinear systems, such as neocortex presents, it is not sensible to simply apply simple mean-field theories which assume sharply peaked distributions, since the dynamics of nonlinear diffusions in particular are typically washed out.

Previous SMNI EEG studies had demonstrated that simple linearized dispersion relations derived from the EL equations support the local generation of frequencies observed experimentally as well as deriving diffusive propagation velocities of information across minicolumns consistent with other experimental studies. The earliest studies simply used a driving force $J_G M^G$ in the Lagrangian to model long-ranged interactions among fibers (Ingber, 1982; Ingber, 1983). Subsequent studies considered regional interactions driving localized columnar activity within these regions (Ingber, 1996b; Ingber, 1997; Ingber, 1998).

A recent set of calculations examined these columnar EL equations to see if EEG oscillatory behavior could be supported at just this columnar scale, i.e., within a single column. At first, the EL equations were quasi-linearized, by extracting coefficients of $M$ and $dM/dt$. The nonlinear coefficients were presented as graphs over all firing states (Ingber, 2009a). This exercise demonstrated that a spring-type model of oscillations was plausible. Then a more detailed study was performed, developing over two million lines of C code from the algebra generated by an algebraic tool, Maxima, to see what range of oscillatory behavior could be considered as optimal solutions satisfying the EL equations (Ingber, 2009b). The answer was affirmative, in that ranges of $\omega t \approx 1$ were supported, implying that oscillatory solutions might be sustainable just due to columnar dynamics at that scale. The full probability distribution was evolved with such oscillatory states, confirming this is true.

These results survive even with oscillatory input into minicolumns from long-ranged sources (Ingber & Nunez, 2010), since the CM is independent of firing states, and just depends on averaged synaptic values used in SMNI.

### 3.4. Macroscopic Computation

Computation in neocortex often includes interactions between information processed at finer scales. For example, it has been noted that experimental data on velocities of propagation of long-ranged fibers (Nunez, 1981; Nunez, 1995) and derived velocities of propagation of information across local minicolumnar interactions (Ingber, 1982) yield comparable times scales of interactions across minicolumns of tenths of a second. Furthermore, since a reasonable case has been made that global EEG is shaped and constrained by geometry of the skull, and since not all information flow across regions need not be direct, it is possible that macroscopic EEG plays a significant role, at least a constraint, on some information processing across regions. Therefore, such phenomena as STM likely are inextricably dependent on interactions at local and global scales, and this is assumed here.

## 4. Microscales

In regard to neocortical information processing at the level of short-term memory (STM), there are two major paradigms that have not yet been reconciled.

### 4.1. Bottom Up

There has been much work done, both experimentally and theoretically, detailing quite a few specific mechanisms at the level of individual neurons and glial processes and their interactions, that can explain information processing and codification of information that may be instrumental in STM (Amzica & Massimini, 2002). In particular, a class of glial cells, astrocytes, present in numbers greater than neurons in human neocortex, is of interest here (Oberheim *et al*, 2009). For example, astrocytes in neocortical laminae 1 extend their mm processes across associative/computing laminae 1-3, afferent laminae 4, touching and communicating with other glia cells and neurons (Reisin & Colombo, 2002; Colombo *et al*, 2005). Laminae 2-6 have larger astrocytes, and in laminae 5-6 with mostly efferent neuronal processes there are some astrocytes with varicose projections (Oberheim *et al*, 2009). However, it appears that a primary means of communication among astrocytes (and other glial cells) is via $Ca^{2+}$ waves, propagating at speeds up to 40 $\mu$m/s (Bellinger, 2005) over hundreds of mm of neuronal structures. They influence excitation and inhibition of neuromodulators, and recent research points to their direct effect on polarization thresholds via $Ca^{2+}$ waves. For example, the influence of neuron firing on astroglial calcium ions may be caused by movement of sodium and potassium ions in and out the body and axon of neurons.

It should be noted that there are other mechanisms proposed, other than direct neuron-neuron interactions, to describe various aspects of neocortical information processing, e.g., soliton formation (Georgiev, 2003), and ephaptic excitation of neurons (Anastassiou *et al*, 2011).

There are many approaches in this "bottom-up" context, including quantum computation in microtubles (Hagan *et al*, 2002), nonlinear systems approaches to neural processes (Rabinovich *et al*, 2006), magnetic processes within astrocytes (Banaclocha, 2005; Banaclocha, 2007; Banaclocha & Banaclocha, 2010; Banaclocha, Bóokkon & Banaclocha, 2010), pulsating $Ca^{2+}$ waves in astrocytes (Schipke *et al*, 2002; Scemes *et al*, 2000; Goldberg *et al*, 2010), neuron-astrocyte networks (Pereira & Furlan, 2009; Pereira & Furlan, 2010), including glutamate-specific $Ca^{2+}$-induced signaling processes between neurons and

astrocytes (Postnov *et al*, 2009), influences of blood flow on neuronal processes (Moore & Cao, 2008), and mathematical formulations of qualia based on neural information processing (Balduzzi & Tononi, 2009).

### 4.2. Top Down

There has been much theoretical work done at the level of columnar and regional neocortical activity, detailing correlations of experimental brain activity with behavioral observations (Buxhoeveden & Casanova, 2002; Rakic, 2008). For example, various imaging techniques, both intra-cranial and non-invasive, have demonstrated that specific brain activity often is correlated with STM as well as specific processing of information and attentional states (Nunez & Srinivasan, 2006).

There also has been much theoretical work trying to bridge brain activity across multiples scales, e.g., from neuronal to columnar to regional scales of activity, with detailed calculations defining STM (Ingber, 1981; Ingber, 1983; Ingber, 1984; Ingber & Nunez, 1995) and analyses of scalp EEG (Ingber, 1997; Ingber, 2009b; Ingber & Nunez, 2010). Relevant to the present work, minicolumnar EEG has been demonstrated to scale up to EEG observed at regional scalp measurements. While minicolumnar EEG may not be the only source of scalp EEG, it is sufficient to scale for detailed fits to observed scalp EEG data.

It is reasonable to state that, while most neuroscientists believe that ultimately Bottom Up processing will explain all brain activity (Rabinovich *et al*, 2006), some other neurophysiologists and psychologists believe that direct Top Down processes are important components of mammalian information processing, which cannot be solely explained by Bottom Up processes.

### 4.3. Smoking Gun

As yet, there does not seem to be any "smoking gun" for explicit Top to Down mechanisms that directly drive Bottom Up STM processes. Of course, there are many Top Down type studies demonstrating that neuromodulator and neuronal firing states, e.g., as defined by EEG frequencies, can modify the milieu or context of individual synaptic and neuronal activity, which is still consistent with ultimate Bottom Up paradigms. However, there is a logical difference between Top Down milieu as conditioned by some prior external or internal conditions, and some direct Top Down processes that direct cause Bottom Up interactions specific to STM. Here, the operative word is "cause".

### 4.4. Support for Top-Down Mechanism

There is a body of evidence that suggests a specific Top to Down mechanism for neocortical STM processing.

#### 4.4.1. Magnetism Influences in Living Systems

An example of a direct physical mechanism that affects neuronal processing not part of "standard" sensory influences is the strong possibility of magnetic influences in birds at quantum levels of interaction (Kominis, 2009; Rodgers & Hore, 2009; Solov'yov & Schulten, 2009). It should be noted that this is just a proposed mechanism (Johnsen & Lohmann, 2008).

#### 4.4.2. Neocortical Magnetic Fields

There are many studies on electric (Alexander *et al*, 2006) and magnetic fields in neocortex (Murakami & Okada, 2006; McFadden, 2007; Irimia *et al*, 2009; Georgiev, 2003).

At the level of a single neuron, electric field strengths can be as high as about 10V/m for a summation of excitatory or inhibitory postsynaptic potentials as a neuron fires. The electric field **D**

$$\mathbf{D} = \varepsilon \mathbf{E} \tag{16}$$

is rapidly attenuated as the dielectric constant $\varepsilon$ seen by ions is close to two orders of magnitude times that in vacuum, $\varepsilon_0$ due to polarization of water (Nunez, 1981). Magnetic field strengths **H** in neocortex are generally quite small, even when estimated for the largest human axons at about $10^{-7}$T, about 1/300 of the Earth's magnetic field, in dendritic microtubles, based on ferrofluid approximation to the microtuble

environment with a magnetic permeability $\mu$,

$$\mathbf{B} = \mu\mathbf{H} \tag{17}$$

about $10\mu_0$ (Georgiev, 2003). Thus, the electromagnetic fields in neocortex differ substantially from those in vacuum, i.e.,

$$\varepsilon_0\mu_0 c^2 = 1 \tag{18}$$

where $c$ is the speed of light.

The above estimates of electric and magnetic field strengths do not consider collective interactions within and among neighboring minicolumns, which give rise to field strengths much larger as typically measured by noninvasive EEG and MEG recordings. While electrical activity may be attenuated in the neocortical environment, this is not true for magnetic fields which may increase collective strengths over relatively large neocortical distances. The strengths of magnetic fields in neocortex may be at a threshold to directly influence synaptic interactions with astrocytes, as proposed for long-term memory (LTM) (Gordon *et al*, 2009) and short-term memory (STM) (Banaclocha, 2007; Pereira & Furlan, 2010) Magnetic strengths associated by collective EEG activity at a columnar level gives rise to even stronger magnetic fields. Columnar excitatory and inhibitory processes largely take place in different neocortical laminae, providing possibilities for more specific mechanisms.

### 4.4.3. Columnar EEG

As discussed above, details of STM have been calculated in the SMNI papers. The Centering Mechanism (CM), associated in these calculations with changes in background inhibitory synaptic activity, drive the columnar system into multiple collective firing states. This CM leads to detailed calculations of STM capacity, duration and stability that agrees with experimental observations.

Future work must consider magnetic fields produced at different laminae due to collective minicolumnar firings as detailed by SMNI for STM processes. These magnetic fields may affect $Ca^{2+}$ ion waves that are considered by some researchers as being vital processes for astrocyte-neural interactions that give rise to higher-order cognitive states (Bellinger, 2005; Nakano *et al*, 2007).

The interactions between the momentum of these $Ca^{2+}$ ions and minicolumnar magnetic fields can be approached classically, e.g., at a local minicolumnar scale, or quantum mechanically, e.g., considering possible entanglement across macrocolumnar scales.

### 4.5. Strengths of Vector Potential

To demonstrate that top-down influences can be appreciable, here a direct comparison is described between the momentum $\mathbf{p}$ of $Ca^{2+}$, ions which already have been established as being influential in STM and LTM, and an SMNI vector potential (SMNI-VP). The SMNI-VP is constructed from magnetic fields induced by neuronal electrical firings, at thresholds of collective minicolumnar activity with laminar specification, which plausibly can give rise to causal top-down mechanisms that effect molecular excitatory and inhibitory processes in STM and LTM. A specific example might be causal influences on momentum $\mathbf{p}$ of $Ca^{2+}$ ions by the SMNI-VP $\mathbf{A}$, as calculated by the canonical momentum $\mathbf{q}$

$$\mathbf{q} = \mathbf{p} - e\mathbf{A} \tag{19}$$

where $e$ is the electron coulomb charge and $\mathbf{B} = \nabla \times \mathbf{A}$ is the magnetic field $\mathbf{B}$, which may be applied either classically or quantum-mechanically. Note that gauge of $\mathbf{A}$ is not specified here, and this can lead to important effects especially at quantum scales (Tollaksen *et al*, 2010).

$\mathbf{A}$ can be calculated using the standard assumption that large-scale EEG is developed from oscillatory electrical dipole activity $\mathbf{p}\exp(-i\omega t)$, the first moment of the charge distribution density $\rho$ giving rise to the dipole. The electromagnetic vector potential $\mathbf{A}$ (Jackson, 1962) is

$$\mathbf{A} = \frac{e^{i\omega r/c}}{cr} \int \mathbf{J} d^3x \tag{20}$$

for the electric current density $\mathbf{J}$, which in the dipole approximation,

$$\mathbf{p} = \int \mathbf{x}\rho(\mathbf{x})d^3x \tag{21}$$

gives rise to

$$\mathbf{A} = -\frac{i\omega\mathbf{p}e^{i\omega r/c}}{cr} \tag{22}$$

This is a dipole model for collective minicolumnar oscillatory currents, corresponding to top-down signaling, flowing in axons, not for individual neurons. The top-down signal is claimed to cause relevant effects on the surrounding milieu, but is not appropriate outside these surfaces due to strong attentuation of electrical activity. However, the vector potentials produced by these dipoles due to axonal discharges do survive far from the axons, and this can lead to important effects at the molecular scale, e.g., in the environment of ions (Feynman *et al*, 1964; Giuliani, 2010).

Note that this is not necessarily the only or most popular description of electromagnetic influences in neocortex, which often describes dendritic presynaptic activity as inducing large scale EEG (Nunez, 1981), or axonal firings directly affecting astrocyte processes (McFadden, 2007). This work is only and specifically concerned with electromagnetic fields in collective axonal firings, directly associated with columnar STM phenomena in SMNI calculations, which create vector potentials influencing ion momenta just outside minicolumnar structures.

After fitting the electrical dipole moment **p** to minicolumnar electrical field near minicolumns, this value of **A** is then to be compared to the value of **p** for $Ca^{2+}$. Note that the magnetic field **B** derived from **A**,

$$\mathbf{B} = \nabla \times \mathbf{A} \tag{23}$$

is still attenuated in the glial areas where $Ca^{2+}$ waves exist, but **A** derived near the minicolumns will be used there as well since it is not so attenuated.

The electrical dipole for collective minicolumnar EEG derived from **A** is

$$\mathbf{E} = \frac{ic}{\omega}\nabla \times \mathbf{B} = \frac{ic}{\omega}\nabla \times \nabla \times \mathbf{A} \tag{24}$$

which in a near-field approximation for minicolumns gives

$$\mathbf{E} = \frac{3\mathbf{n}(\mathbf{n}\cdot\mathbf{p}) - \mathbf{p}}{r^3}$$

$$\mathbf{B} = \frac{i\omega\mathbf{n}\times\mathbf{p}}{cr^2} \tag{25}$$

where **n** is the unit vector in the direction of **p**. The far-field approximations are

$$\mathbf{E} = \mathbf{B}\times\mathbf{n}$$

$$\mathbf{B} = \frac{\omega^2\mathbf{n}\times\mathbf{p}e^{i\omega r/c}}{(cr)^2} \tag{26}$$

The SMNI columnar probability distributions, derived from statistical aggregation of synaptic and neuronal interactions among minicolumns and macrocolumns, have established credibility at columnar scales by detailed calculations of properties of STM. Under CM conditions, they exhibit multiple columnar collective firing states. It must be stressed that these minicolumns are the entities which the above dipole moment is modeling. The Lagrangian of the SMNI distributions, although possessing multivariate nonlinear means and covariance, have functional forms similar to arguments of firing distributions of individual neurons, so that the description of the columnar dipole above is a model faithful to the standard derivation of a vector potential from an oscillating electric dipole.

The effective collective minicolumnar potential is estimated to be about 10 times as strong as a neuronal postsynaptic voltage of $10^{-3}V$, or $10^{-2}$ V, where V measures volts, equivalent to $m^2$-kg-/A-$s^3$ (A measures amperes). At a laminar thickness, $r$, within axons, of about $10^{-3}$ m, the **E** field density dimension is on the order of $10^{-2}/r$ V/m. This gives a dipole value on the order of $10^{-2}r^2$ C-m (C measures coulomb,

measured by A-s) at the near field.

This yields an estimate for values of $|\mathbf{A}|$, for $\omega = 6.366$ cps, corresponding to EEG frequencies of 40 $s^{-1}$ A-s/$m^2$, on the order of $10^{-10}r$ V-m at the near field of firing minicolumns. In SI units, as can be described by the Coulomb force, the equivalent units of C = (kg-$m^3/s^2$)$^{1/2}$, or $eA$ will be in units of linear momentum. Taking $r$ to be a laminae thickness gives an estimate of $10^{-13}$ V-m, which decreases as $1/r$ away from the near field, all measured within axons for the purposes of describing electrical activity.

The contribution of $\mathbf{A}$ to the canonical momentum is measured by $e\mathbf{A}$, where $e = 1.602 \times 10^{-19}$ C. This gives a momentum contribution from $\mathbf{A}$ on the order of $10^{-32}$ kg-m/s.

The mass of a $Ca^{2+}$ ion is $1.33 \times 10^{-25}$ kg. Assuming speeds of 40 $\mu$m/s, estimate the momentum of a single ion is estimated to be about $5 \times 10^{-30}$ kg-m/s.

This comparison of $\mathbf{p}$ and $\mathbf{A}$ demonstrates it is possible for minicolumnar electromagnetic fields to influence important ions involved in cognitive and affective processes in neocortex. Our estimate of minicolumnar electric dipole is quite conservative, and a factor of 10 would make these effects even more dramatic. Since this effect acts on all $Ca^{2+}$ ions, it may have an even greater effect on $Ca^{2+}$ waves, contributing to their mean wave-front movement. Considering slower ion momenta $\mathbf{p}$ would make this comparison to $\mathbf{A}$ even closer.

Such a smoking gun for top-down effects awaits forensic in vivo experimental verification, requiring appreciating the necessity and due diligence of including true multiple-scale interactions across orders of magnitude in the complex neocortical environment.

### 4.6. Microscopic Computation

This work simply shows that electromagnetic fields within neurons can have effects outside of them, e.g., on ions that mediate interactions between and among neurons and astrocytes (Pereira & Furlan, 2010; Pereira & Furlan, 2009). Other work has shown the important computational effects of such interactions, including consideration of magnetic influences per se (Banaclocha, 2007; Banaclocha, Bóokkon & Banaclocha, 2010).

## 5. Conclusion

This paper has focused on some specific approaches, like SMNI and the vector potential of minicolumnar electromagnetic activity, to delve into influences of neocortical interactions and their possible influences on cognitive processing, at multiple scales. Even within this confined context, a case has been made that it should not be expected that the proposed Holy Grail of neuroscience, i.e., to ultimately explain all brain processing in terms of a nonlinear science at molecular scales (Rabinovich *et al*, 2006), is at all realistic. As with many Crusades for some truths, other truths can be trampled. There is much more work to be done on STM at multiple scales (Ingber, 2012).

## Acknowledgments

I thank Alfredo Pereira Jr and Marcos Banaclocha for several discussions and for references to relevant literature on astrocyte processes. I thank Paul Nunez for several discussions on electrical and magnetic fields in neocortex.

**References**


Alexander, J.K., Fuss, B. & Colello, R.J. (2006) Electric field-induced astrocyte alignment directs neurite outgrowth. Neuron Glia Biology. 2(2), 93-103.

Amzica, F. & Massimini, M. (2002) Glial and neuronal interactions during slow wave and paroxysmal activities in the neocortex. Cerbral Cortex. 12(10), 1101-1113.

Anastassiou, C.A., Perin, R., Markram, H. & Koch, C. (2011) Ephaptic coupling of cortical neurons. Nature Neuroscience. 14, 217-223.

Arbib, M.A. & Amari, S.-I. (1985) Sensori-motor transformations in the brain (with a critique of the tensor theory of cerebellum). Journal of Theoretical Biology. 112, 123-155.

Balduzzi, D. & Tononi, G. (2009) Qualia: The geometry of integrated information. PLoS Computational Biology. 5(8), 1-24.

Banaclocha, M.A.M. (2005) Magnetic storage of information in the human cerebral cortex: A hypothesis for memory. International Journal of Neuroscience. 115(3), 329-337.

Banaclocha, M.A.M. (2007) Neuromagnetic dialogue between neuronal minicolumns and astroglial network: A new approach for memory and cerebral computation. Brain Research Bulletin. 73, 21-27.

Banaclocha, M.A.M. & Banaclocha, H.M. (2010) Spontaneous neocortical activity and cognitive functions: A neuron-astroglial bio-magnetic and self-organized process. NeuroQuantology. 8(2), 191-199.

Banaclocha, M.A.M., Bóokkon, I. & Banaclocha, H.M. (2010) Long-term memory in brain magnetite. Medical Hypotheses. 74(2), 254-257.

Bellinger, S. (2005) Modeling calcium wave oscillations in astrocytes. Neurocomputing. 65(66), 843-850.

Buxhoeveden, D.P. & Casanova, M.F. (2002) The minicolumn hypothesis in neuroscience. Brain. 125(5), 935-951. [URL http://tinyurl.com/bc2002brain]

Colombo, J.A., Reisin, H.D., Jones, M. & Bentham, C. (2005) Development of interlaminar astroglial processes in the cerebral cortex of control and Down's syndrome human cases. Experimental Neurology. 193, 207-217.

Ericsson, K.A. & Chase, W.G. (1982) Exceptional memory. American Scientist. 70, 607-615.

Feynman, R.P., Leighton, R.B. & Sands, M. (1964) Chapter 15: The Vector Potential, In: The Feynman Lectures on Physics, Addison-Wesley, 1-16.

Georgiev, D. (2003) Electric and magnetic fields inside neurons and their impact upon the cytoskeletal microtubules. Cogprints Report. Cogprints. [http://cogprints.org/3190/]

Giuliani, G. (2010) Vector potential, electromagnetic induction and 'physical meaning'. European Journal of Physics. 31(4), 871-880.

Goldberg, M., Pittà, M. De, Volman, V., Berry, H. & Ben-Jacob, E. (2010) Nonlinear Gap Junctions Enable Long-Distance Propagation of Pulsating Calcium Waves in Astrocyte Networks. PLoS Computational Biology. 6(8), 1-14.

Gordon, G.R.J., Iremonger, K.J., Kantevari, S., Ellis-Davies, G.C.R., MacVicar, B.A. & Bains, J.S. (2009) Astrocyte-mediated distributed plasticity at hypothalamic glutamate synapses. Neuron. 64, 391-403.

Graham, R. (1977) Covariant formulation of non-equilibrium statistical thermodynamics. Zeitschrift für Physik. B26, 397-405.

Graham, R. (1978) Path-integral methods in nonequilibrium thermodynamics and statistics, In: Stochastic Processes in Nonequilibrium Systems, ed. L. Garrido, P. Seglar & P.J. Shepherd. Springer, 82-138.

Grossberg, S. (1983) The quantized geometry of visual space: The coherent computation of depth, form, and lightness. Behav. Brain Sci.. 6, 625-692.

Hagan, S., Hameroff, R. & Tuszyński, J.A. (2002) Quantum computation in brain microtubules: Decoherence and biological feasibility. Physical Review E. 65(061901), 1-11.

Ingber, L. (1981) Towards a unified brain theory. Journal Social Biological Structures. 4, 211-224. [URL http://www.ingber.com/smni81_unified.pdf]

Ingber, L. (1982) Statistical mechanics of neocortical interactions. I. Basic formulation. Physica D. 5, 83-107. [URL http://www.ingber.com/smni82_basic.pdf]

Ingber, L. (1983) Statistical mechanics of neocortical interactions. Dynamics of synaptic modification. Physical Review A. 28, 395-416. [URL http://www.ingber.com/smni83_dynamics.pdf]

Ingber, L. (1984) Statistical mechanics of neocortical interactions. Derivation of short-term-memory capacity. Physical Review A. 29, 3346-3358. [URL http://www.ingber.com/smni84_stm.pdf]

Ingber, L. (1985a) Statistical mechanics algorithm for response to targets (SMART), In: Workshop on Uncertainty and Probability in Artificial Intelligence: UC Los Angeles, 14-16 August 1985, American Association for Artificial Intelligence, 258-264. [URL http://www.ingber.com/combat85_smart.pdf]

Ingber, L. (1985b) Statistical mechanics of neocortical interactions. EEG dispersion relations. IEEE Transactions Biomedical Engineering. 32, 91-94. [URL http://www.ingber.com/smni85_eeg.pdf]

Ingber, L. (1985c) Statistical mechanics of neocortical interactions: Stability and duration of the 7+-2 rule of short-term-memory capacity. Physical Review A. 31, 1183-1186. [URL http://www.ingber.com/smni85_stm.pdf]

Ingber, L. (1986) Statistical mechanics of neocortical interactions. Bulletin American Physical Society. 31, 868.

Ingber, L. (1991) Statistical mechanics of neocortical interactions: A scaling paradigm applied to electroencephalography. Physical Review A. 44(6), 4017-4060. [URL http://www.ingber.com/smni91_eeg.pdf]

Ingber, L. (1992) Generic mesoscopic neural networks based on statistical mechanics of neocortical interactions. Physical Review A. 45(4), R2183-R2186. [URL http://www.ingber.com/smni92_mnn.pdf]

Ingber, L. (1993) Adaptive Simulated Annealing (ASA). Global optimization C-code. Caltech Alumni Association. [URL http://www.ingber.com/#ASA-CODE]

Ingber, L. (1994) Statistical mechanics of neocortical interactions: Path-integral evolution of short-term memory. Physical Review E. 49(5B), 4652-4664. [URL http://www.ingber.com/smni94_stm.pdf]

Ingber, L. (1995a) Statistical mechanics of multiple scales of neocortical interactions, In: Neocortical Dynamics and Human EEG Rhythms, ed. P.L. Nunez. Oxford University Press, 628-681. [ISBN 0-19-505728-7. URL http://www.ingber.com/smni95_scales.pdf]

Ingber, L. (1995b) Statistical mechanics of neocortical interactions: Constraints on 40 Hz models of short-term memory. Physical Review E. 52(4), 4561-4563. [URL http://www.ingber.com/smni95_stm40hz.pdf]

Ingber, L. (1996a) Nonlinear nonequilibrium nonquantum nonchaotic statistical mechanics of neocortical interactions. Behavioral and Brain Sciences. 19(2), 300-301. [Invited commentary on Dynamics of the brain at global and microscopic scales: Neural networks and the EEG, by J.J. Wright and D.T.J. Liley. URL http://www.ingber.com/smni96_nonlinear.pdf]

Ingber, L. (1996b) Statistical mechanics of neocortical interactions: Multiple scales of EEG, In: Frontier Science in EEG: Continuous Waveform Analysis (Electroencephalography Clinical Neurophysiology Suppl. 45), ed. R.M. Dasheiff & D.J. Vincent. Elsevier, 79-112. [Invited talk to Frontier Science in EEG Symposium, New Orleans, 9 Oct 1993. ISBN 0-444-82429-4. URL http://www.ingber.com/smni96_eeg.pdf]

Ingber, L. (1997) Statistical mechanics of neocortical interactions: Applications of canonical momenta indicators to electroencephalography. Physical Review E. 55(4), 4578-4593. [URL http://www.ingber.com/smni97_cmi.pdf]

Ingber, L. (1998) Statistical mechanics of neocortical interactions: Training and testing canonical momenta indicators of EEG. Mathematical Computer Modelling. 27(3), 33-64. [URL http://www.ingber.com/smni98_cmi_test.pdf]

Ingber, L. (2000) High-resolution path-integral development of financial options. Physica A. 283(3-4), 529-558. [URL http://www.ingber.com/markets00_highres.pdf]

Ingber, L. (2005) Trading in Risk Dimensions (TRD). Report 2005:TRD. Lester Ingber Research. [URL http://www.ingber.com/markets05_trd.pdf]

Ingber, L. (2006) Ideas by statistical mechanics (ISM). Report 2006:ISM. Lester Ingber Research. [URL http://www.ingber.com/smni06_ism.pdf]

Ingber, L. (2007) Ideas by Statistical Mechanics (ISM). Journal Integrated Systems Design and Process Science. 11(3), 31-54. [Special Issue: Biologically Inspired Computing.]

Ingber, L. (2008) AI and Ideas by Statistical Mechanics (ISM), In: Encyclopedia of Artificial Intelligence, ed. J.R. Rabuñal, J. Dorado & A.P. Pazos. Information Science Reference, 58-64. [ISBN 978-1-59904-849-9]

Ingber, L. (2009a) Statistical mechanics of neocortical interactions: Columnar EEG. Report 2009:CEEG. Lester Ingber Research. [URL http://www.ingber.com/smni09_columnar_eeg.pdf]

Ingber, L. (2009b) Statistical mechanics of neocortical interactions: Nonlinear columnar electroencephalography. NeuroQuantology Journal. 7(4), 500-529. [URL http://www.ingber.com/smni09_nonlin_column_eeg.pdf]

Ingber, L. (2012) Columnar EEG magnetic influences on molecular development of short-term memory, In: Short-Term Memory: New Research, ed. N. Gotsiridze-Columbus. Nova, (to be published). [Invited Paper]

Ingber, L., Chen, C., Mondescu, R.P., Muzzall, D. & Renedo, M. (2001) Probability tree algorithm for general diffusion processes. Physical Review E. 64(5), 056702-056707. [URL http://www.ingber.com/path01_pathtree.pdf]

Ingber, L., Fujio, H. & Wehner, M.F. (1991) Mathematical comparison of combat computer models to exercise data. Mathematical Computer Modelling. 15(1), 65-90. [URL http://www.ingber.com/combat91_data.pdf]

Ingber, L. & Nunez, P.L. (1990) Multiple scales of statistical physics of neocortex: Application to electroencephalography. Mathematical Computer Modelling. 13(7), 83-95.

Ingber, L. & Nunez, P.L. (1995) Statistical mechanics of neocortical interactions: High resolution path-integral calculation of short-term memory. Physical Review E. 51(5), 5074-5083. [URL http://www.ingber.com/smni95_stm.pdf]

Ingber, L. & Nunez, P.L. (2010) Neocortical Dynamics at Multiple Scales: EEG Standing Waves, Statistical Mechanics, and Physical Analogs. Mathematical Biosciences. 229, 160-173. [doi:10.1016/j.mbs.2010.12.003 URL http://www.ingber.com/smni10_multiple_scales.pdf]

Irimia, A., Swinney, K.R. & Wikswo, J.P. (2009) Partial independence of bioelectric and biomagnetic field and its implications for encephalography and cardiography. Physical Review E. 79(051908), 1-13.

Jackson, J.D. (1962) Classical Electrodynamics. Wiley & Sons, New York.

Jirsa, V.K. & Haken, H. (1996) Field theory of electromagnetic brain activity. Physical Review Letters. 77(5), 960-963.

Johnsen, S. & Lohmann, K.L. (2008) Magnetoreception in animals. Physics Today. 61, 29-35.

Kominis, I.K. (2009) Zeno is pro Darwin: quantum Zeno effect suppresses the dependence of radical-ion-pair reaction yields on exchange and dipolar interactions. arXiv:0908.0763v2 [quant-ph]. University of Crete.

Langouche, F., Roekaerts, D. & Tirapegui, E. (1979) Discretization problems of functional integrals in phase space. Physical Review D. 20, 419-432.

Langouche, F., Roekaerts, D. & Tirapegui, E. (1982) Functional Integration and Semiclassical Expansions. Reidel, Dordrecht, The Netherlands.

McFadden, J. (2007) Conscious electromagnetic field theory. NeuroQuantology. 5(3), 262-270.

Miller, G.A. (1956) The magical number seven, plus or minus two. Psychology Review. 63, 81-97.

Moore, C.I. & Cao, R. (2008) The hemo-neural hypothesis: On the role of blood flow in information processing. Journal of Neurophysiology. 99, 2035-2047.

Mountcastle, V.B. (1978) An organizing principle for cerebral function: The unit module and the distributed system, In: The Mindful Brain, ed. G.M. Edelman & V.B. Mountcastle. Massachusetts Institute of Technology, 7-50.

Mountcastle, V.B., Andersen, R.A. & Motter, B.C. (1981) The influence of attentive fixation upon the excitability of the light-sensitive neurons of the posterior parietal cortex. Journal of Neuroscience. 1, 1218-1235.

Murakami, S. & Okada, Y. (2006) Contributions of principal neocortical neurons to magnetoencephalography and electroencephalography signals. Journal of Physiology. 575(3), 925-936.

Nakano, T., Suda, T., Koujin, T., Haraguchi, T. & Hiraoka, Y. (2007) Molecular communication through gap junction channels: System design, experiments and modeling, In: Proceedings 2nd International Conference on Bio-Insprired Models of Network, Information, and Computing Systems, Institute for Computer Sciences, Social-Informatics and Telecommunications Engineering, 139-146.

Naruse, Y., Matani, A., Miyawaki, Y. & Okada, M. (2009) Influence of coherence between multiple cortical columns on alpha rhythm: A computational modeling study. Human Brain Mapping. 31(5), 703-715.

Nunez, P.L. (1981) Electric Fields of the Brain: The Neurophysics of EEG. Oxford University Press, London.

Nunez, P.L. (1989) Generation of human EEG rhythms by a combination of long and short-range neocortical interactions. Brain Topography. 1, 199-215.

Nunez, P.L. (1995) Neocortical Dynamics and Human EEG Rhythms. Oxford University Press, New York, NY.

Nunez, P.L. & Srinivasan, R. (2006) Electric Fields of the Brain: The Neurophysics of EEG, 2nd Ed.. Oxford University Press, London.

Oberheim, N.A., Takano, T., Han, X., He, W., Lin, J.H.C., Wang, F., Xu, Q., Wyatt, J.D., Pilcher, W., Ojemann, J.G., Ransom, B.R., Goldman, S.A. & Nedergaard, M. (2009) Uniquely hominid features of adult human astrocytes. Journal of Neuroscience. 29(10), 3276-3287.

Pereira, A., Jr. & Furlan, F.A. (2009) On the role of synchrony for neuron-astrocyte interactions and perceptual conscious processing. Journal of Biological Physics. 35(4), 465-480.

Pereira, A., Jr. & Furlan, F.A. (2010) Astrocytes and human cognition: Modeling information integration and modulation of neuronal activity. Progress in Neurobiology. 92, 405-420.

Postnov, D.E., Koreshkov, R.N., Brazhe, N.A., Brazhe, A.R. & Sosnovtseva, O.V. (2009) Dynamical patterns of calcium signaling in a functional model of neuron-astrocyte networks. Journal of Biological Physics. 35, 425-445.

Rabinovich, M.I., Varona, P., Selverston, A.I. & Arbaranel, H.D.I. (2006) Dynamical principles in neuroscience. Reviews Modern Physics. 78(4), 1213-1265.

Rakic, P. (2008) Confusing cortical columns. Proceedings of the National Academy of Sciences. 105(34), 12099-12100. [URL http://www.pnas.org/content/105/34/12099.full]

Reisin, H.D. & Colombo, J.A. (2002) Considerations on the astroglial architecture and the columnar organization of the cerebral cortex. Cellular and Molecular Neurobiology. 22(5/6), 633-644.

Rodgers, C.T. & Hore, P.J. (2009) Chemical magnetoreception in birds: The radical pair mechanism. Proceedings of the National Academy of Sciences. 106(2), 353-360.

Scemes, E., Suadicani, S.O. & Spray, D.C. (2000) Intercellular calcium wave communication via gap junction dependent and independent mechanisms, In: Current Topics in Membranes, Academic Press, 145-173.

Schipke, C.G., Boucsein, C., Ohlemeyer, C., Kirchhoff, F. & Kettenmann, H. (2002) Astrocyte Ca2+ waves trigger responses in microglial cells in brain slices. Federation of American Societies for Experimental Biology Journal. 16, 255-257.

Solov'yov, I.A. & Schulten, K. (2009) Magnetoreception through cryptochrome may involve superoxide. Biophysical Journal. 96(12), 4804-4813.

Tollaksen, J., Aharonov, Y., Casher, A., Kaufherr, T. & Nussinov, S. (2010) Quantum interference experiments, modular variables and weak measurements. New Journal of Physics. 12(013023), 1-29.

Zhang, G. & Simon, H.A. (1985) STM capacity for Chinese words and idioms: Chunking and acoustical loop hypotheses. Memory & Cognition. 13, 193-201.